Article

Cite This: Biomacromolecules 2019, 20, 2913−2921

pubs.acs.org/Biomac

# Alendronate-Functionalized Poly(2-oxazoline)s with Tunable Affinity for Calcium Cations

María J. Sánchez-Fernández,[†,‡] Mikey R. Immers,[†] Rosa P. Félix Lanao,[†] Fang Yang,[‡] Johan C. M. E. Bender,[§] Jasmin Mecinović,[†,#] Sander C. G. Leeuwenburgh,[*,‡,⊥] and Jan C. M. van Hest[*,†,∥,⊥]

[†]Department of Bio-Organic Chemistry, Institute for Molecules and Materials, Radboud University, 6525 AJ Nijmegen, the Netherlands

[‡]Department of Regenerative Biomaterials, Radboudumc, 6525 EX Nijmegen, the Netherlands

[§]GATT Technologies BV, 6525 ED Nijmegen, the Netherlands

[∥]Department of Bio-Organic Chemistry, Institute for Complex Molecular Systems, Eindhoven University of Technology, 5600 MB Eindhoven, the Netherlands

Supporting Information

**ABSTRACT:** A library of poly(2-oxazoline)s functionalized with controllable amounts of alendronate, hydroxyl, and carboxylic acid side groups was successfully synthesized to create novel polymers with tunable affinity for calcium cations. The affinity of alendronate-containing polymers for calcium cations was quantified using isothermal titration calorimetry. Thermodynamic measurements revealed that the $Ca^{2+}$-binding affinity of these polymers increased linearly with the amount of alendronate functionalization, up to values ($K_{Ca}^{2+}$ = 2.4 × $10^5$ $M^{-1}$) that were about 120-fold higher than those for previously reported polymers. The calcium-binding capacity of alendronate-functionalized poly(2-oxazoline)s was exploited to form robust hydrogel networks cross-linked using reversible physical bonds. Oscillatory rheology showed that these hydrogels recovered more than 100% of their initial storage modulus after severe network destruction. The versatile synthesis of alendronate-functionalized polymers and their strong and tunable affinity for calcium cations render these polymers promising candidates for various biomedical applications.

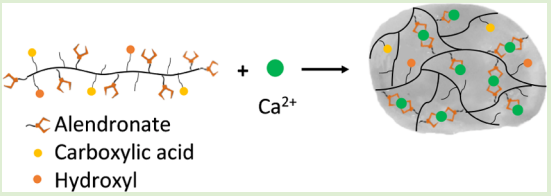


## 1. INTRODUCTION

The synthesis of poly(2-oxazoline)s (POxs) was first reported in the 1960s by four independent groups.[1−4] POxs are synthesized in a well-defined and straightforward manner via cationic ring-opening polymerization (CROP) of functionalized 2-oxazolines. These polymers present a narrow molecular weight distribution, tunable properties, excellent biocompatibility, stealth behavior, stimulus-responsiveness, and versatile functionalization possibilities.[5−7] In recent years, POxs have been established as an alternative to poly(ethylene glycol) (PEG), one of the most widespread polymers used in biomedicine.[8−10] The major advantage of POx over PEG is that the side chains of POx can be easily modified along the entire polymeric backbone and not only at the end groups, which allows for much higher degrees of functionalization.[11,12] This chemical versatility creates many new opportunities for the development of POx-based biomaterials.

Bisphosphonates (BPs) are a class of drugs used to treat several skeletal disorders, including osteoporosis, Paget's disease, and bone metastasis.[13−16] Generally, BP groups such as alendronate (Ale) show a strong affinity for hydroxyapatite, the mineral component of bone tissue.[17−19] This binding affinity is attributed to noncovalent bonds that are formed between the negatively charged BP groups and positively charged calcium ions present at the surface of hydroxyapatite.[20] These electrostatic interactions are reversible, thus allowing the construction of materials with self-healing properties.[20−22] Self-healing materials possess the ability to recover their original mechanical properties after mechanical damage.[23] Recently, research on the development of self-healing materials for biomedical applications has gained significant interest.[24−26] Notably, bisphosphonate-modified self-healing biomaterials with a strong affinity for calcium cations were reported to be highly appealing for bone regenerative applications.[22,27]

Herein, we exploit the chemical versatility of POx to synthesize a novel library of alendronate-functionalized POxs (POx-Ale) with tunable calcium-binding affinity. To this end, these polymers were chemically functionalized with alendronate as well as carboxylic acid and hydroxyl side groups. To enable the formation of robust hydrogels consisting of networks of calcium-cross-linked POx-Ale polymers, these polymers should meet several requirements. First, POx-Ale polymers should comprise sufficient reactive moieties to allow for cross-linking with calcium cations. Second, the side chains presenting the

Received: January 22, 2019
Revised: March 19, 2019
Published: July 31, 2019




DOI: 10.1021/acs.biomac.9b00104
Biomacromolecules 2019, 20, 2913−2921

**Scheme 1. Synthetic Route of POx-Ale. The End Groups Depicted as * are Similar to the Functionalized Side Chains Shown in Each Reaction Step**

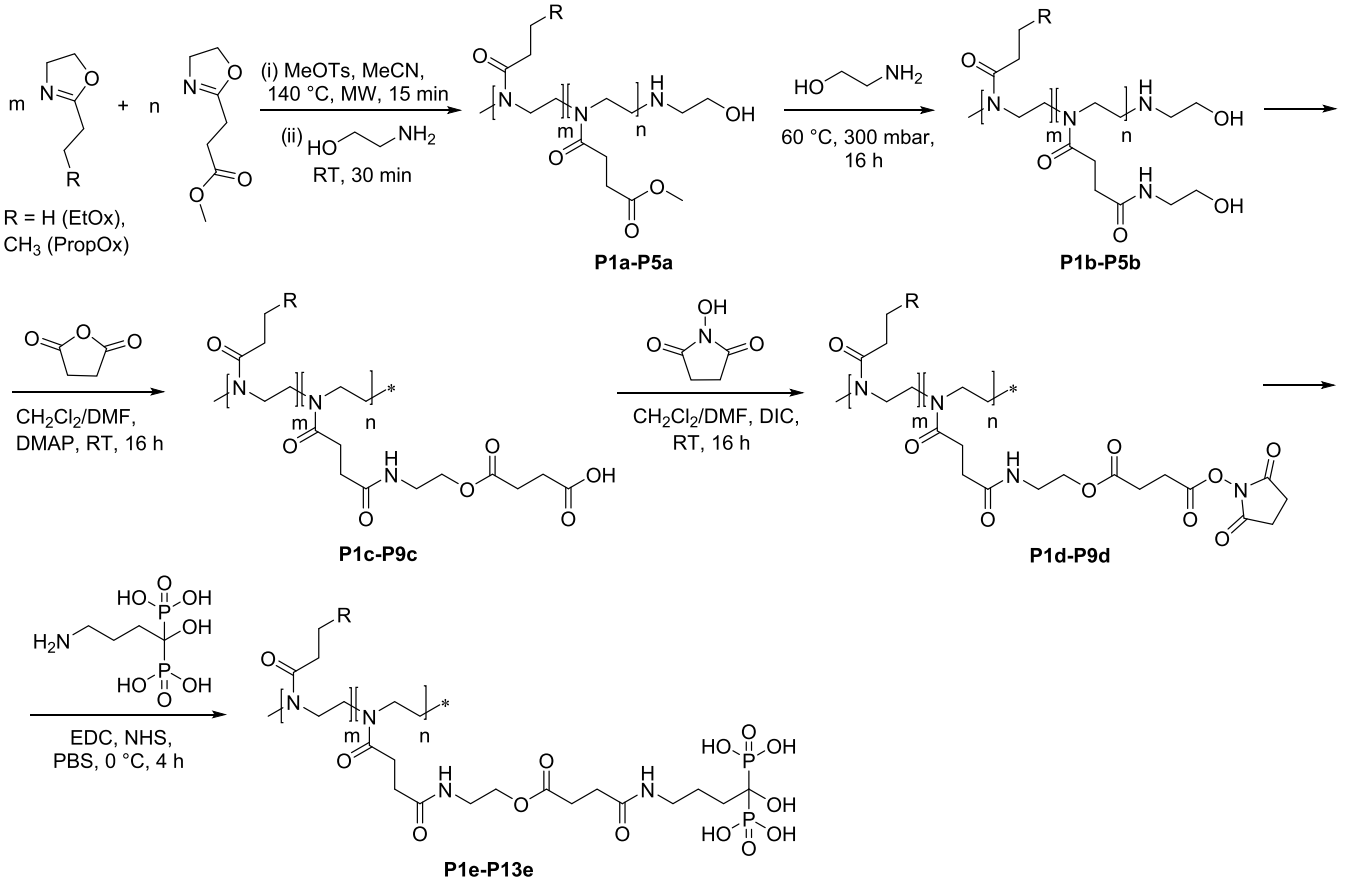


reactive calcium-binding groups should be flexible and long enough to enable the formation of sufficient cross-links. Third, the polymers should be sufficiently polar to be water-soluble and functional under physiological conditions. Therefore, we first studied the binding affinity of our POx-Ale polymers for $Ca^{2+}$ as a function of the type and amount of side groups using isothermal titration calorimetry (ITC). To study the formation, destruction, and self-healing properties of calcium-cross-linked POx-Ale networks, we subsequently characterized their viscoelastic properties, including their self-healing capacity, using oscillatory rheology.

## 2. EXPERIMENTAL SECTION

**2.1. Materials.** 2-Propyl-2-oxazoline (PropOx) and 2-methoxycarbonylethyl-2-oxazoline (MestOx) were kindly provided by GATT Technologies BV. Anhydrous dichloromethane, anhydrous diethyl ether, HPLC-grade methanol, and fused calcium chloride were purchased from Fisher Scientific. Anhydrous *N*,*N*-dimethylformamide was acquired from Acros Organics. Dowex 50WX4 100−200 (H) and succinic anhydride were obtained from Alfa Aesar. *N*-(3-Dimethylaminopropyl)-*N*′-ethylcarbodiimide hydrochloride (EDC), 4-dimethylamino pyridine (DMAP), *N*,*N*′-diisopropylcarbodiimide (DIC), *N*-hydroxysuccinimide (NHS), and sodium alendronate trihydrate (Ale) were acquired from Fluorochem. Amaranth (dye content 85−95%), Brilliant Blue R (dye content 50%), dimethyl sulfoxide, 2-ethanolamine, methyl-*p*-toluenesulfonate (MeOTs), and α-cyano-4-hydroxycinnamic acid (CHCA) were purchased from Sigma-Aldrich. Deuterated solvents as deuterium oxide, chloroform-*d*, and dimethyl sulfoxide-$d_6$ were purchased from Cambridge Isotope Laboratories and Sigma-Aldrich. Dialysis membranes, Spectra/Por 3 (3.5 kDa cutoff), were acquired from VWR International. Sodium chloride, potassium chloride, disodium hydrogen phosphate, and potassium dihydrogen phosphate were obtained from Merck. Reagents were used without purification, except for 2-ethyl-2-oxazoline (EtOx), methyl-*p*-toluenesulfonate (MeOTs), and 2-ethanolamine, which were distilled before use at 40 mbar and 40, 55, and 75 °C, respectively. MeCN and tetrahydrofuran (THF) were discharged under a nitrogen atmosphere using an MBraun MB SPS-800 solvent dispersing system. Ultrapure Milli-Q water set to 18.2 MΩ/cm was obtained from a WaterPro PS polisher. Phosphate-buffered saline (PBS) solution was prepared containing 2.7 mM KCl, 137 mM NaCl, 2 mM $KH_2PO_4$, and 8 mM $Na_2HPO_4$ (pH = 7.4).

**2.2. Synthesis of Alendronate-Functionalized Poly(2-oxazoline)s.** The synthetic route of alendronate-functionalized POxs is based on five steps (Scheme 1):

*2.2.1. Polymerization: Synthesis of Methyl Ester-Functionalized Polymers **P1a−P5a**.* Methyl-*p*-toluenesulfonate (1 equiv), either EtOx (*m* equiv) or PropOx (*m* equiv), MestOx (*n* equiv), and dry MeCN (4 M) were mixed under an inert atmosphere in the desired ratios in microwave vials. The polymerization was carried out under microwave irradiation at 140 °C for 15 min followed by CROP.[28] After polymerization, the reaction was terminated by the addition of 2-ethanolamine (10 equiv) while stirring for 30 min at room temperature. Then, the solvent was removed in vacuo to afford either P(EtOx-*r*-MestOx) or P(PropOx-*r*-MestOx) **P1a−P5a** as statistical copolymers with near-random monomer distribution in the desired ratios.

*2.2.2. Amidation Reaction: Synthesis of Hydroxyl-Functionalized Polymers **P1b−P5b**.* The MestOx-functionalized copolymers **P1a−P5a** (1 equiv) were modified by direct amidation with 2-ethanolamine (3.5 equiv) at 60 °C under reduced pressure (300 mbar) for 16 h. Then, the crude mixtures were purified by three consecutive precipitations in a mixture of acetone/$Et_2O$, 3:1, and subsequent re-dissolution in $CH_2Cl_2$/MeOH, 8:2, followed by ion-exchange chromatography in MeOH. Finally, the solvents were removed in vacuo to afford either


DOI: 10.1021/acs.biomac.9b00104
Biomacromolecules 2019, 20, 2913−2921

P(EtOx-*r*-OH) or P(PropOx-*r*-OH) **P1b−P5b** as statistical copolymers with near-random monomer distribution in the desired ratios.

*2.2.3. Succinic Anhydride Coupling: Synthesis of Carboxylic Acid-Functionalized Polymers **P1c−P9c**.* Hydroxyl side-functionalized polymers **P1b−P5b** (1 equiv) were dissolved in $CH_2Cl_2$/DMF, (9:1, 2 M), under an argon atmosphere and were either fully or partially converted to carboxylic acid moieties using succinic anhydride (1.1 equiv) and 4-dimethylamino pyridine (DMAP, 1.1 equiv) by stirring the mixture for 16 h at room temperature. The crude mixtures were purified by three consecutive precipitations in acetone and subsequent re-dissolution in $CH_2Cl_2$/MeOH, 8:2, followed by ion-exchange chromatography in MeOH. Finally, the solvent was removed in vacuo to afford either P(EtOx/PropOx-*r*-COOH) or P(EtOx/PropOx-*r*-OH-*r*-COOH) **P1c−P9c** as statistical copolymers with near-random monomer distribution in the desired ratios.

*2.2.4. Carbodiimide Reaction: Synthesis of N-Hydroxysuccinimide-Functionalized Polymers **P1d−P9d**.* Carboxyl-functionalized polymers **P1c−P9c** were subsequently modified into reactive esters by carbodiimide coupling with NHS, to facilitate the next amidation reaction. The functionalized polymers were dissolved in $CH_2Cl_2$/DMF (95:5, 0.2 M), *N*-hydroxysuccinimide (NHS, 1.1 equiv) and *N*,*N*′-diisopropylcarbodiimide (DIC, 1.2 equiv) were added as coupling agents, and the mixture was stirred under an argon atmosphere at room temperature for 16 h. The polymers were purified by two precipitations in acetone/$Et_2O$, 1:1, followed by another precipitation in $Et_2O$ and subsequent re-dissolution in $CH_2Cl_2$. Finally, the solvents were removed in vacuo to afford P(EtOx/PropOx-*r*-OH-*r*-NHS) or P(EtOx/PropOx-*r*-NHS) **P1d−P9d** as statistical copolymers with near-random monomer distribution in the desired ratios.

*2.2.5. Amidation Reaction: Synthesis of Alendronate-Functionalized Polymers **P1e−P13e**.* Finally, alendronate moieties were incorporated in the polymer side chain by an amidation reaction. The NHS-activated copolymers **P1d−P9d** (1 equiv) were slowly added into a solution containing sodium alendronate trihydrate (2 equiv), NHS (1 equiv), and *N*-(3-dimethylaminopropyl)-*N*′-ethylcarbodiimide hydrochloride (EDC, 1 equiv) in PBS (0.5 M). NHS and EDC were added to maximize the conversion from NHS- to alendronate-functionalized polymers. The reaction mixtures were stirred at 3 °C for 4 h with the pH adjusted to 7.4−8.0 using NaOH (0.5 M). Afterward, the crude mixtures were purified by three consecutive precipitations in acetone/$Et_2O$, 3:1, and subsequent re-dissolution in Milli-Q water, followed by dialysis using Spectra/Por 3 membranes (3.5 kDa cutoff) for 16 h. Finally, they were lyophilized to afford either P(EtOx/PropOx-*r*-Ale), P(EtOx/PropOx-*r*-OH-*r*-Ale), or P(EtOx/PropOx-*r*-COOH-*r*-Ale) **P1e−P13e** as statistical copolymers with near-random monomer distribution in the desired ratios.

**2.3. Characterization of Alendronate-Functionalized Poly(2-oxazoline)s.** The degree of modification of the different substitutions in the polymers was determined by $^1$H NMR and $^{31}$P NMR spectroscopy. NMR spectra were recorded on a Varian Inova 400 (400 MHz) or Bruker Avance III (400 MHz) spectrometer in the indicated solvent at 25 °C. $^1$H NMR data are reported as chemical shifts (given in parts per million (ppm) with respect to tetramethylsilane as standard), multiplicity (br = broad), integration, and assignment. The standard deviation of quantifications obtained using $^1$H NMR was typically below 1%, which confirms the accuracy of this method.

The average molecular weights ($M_n$) were recorded on a Bruker Microflex LRF matrix-assisted laser desorption ionization time-of-flight mass spectrometry (MALDI-TOF MS) system. All mass spectra were obtained in the positive ion mode. α-Cyano-4-hydroxycinnamic acid (CHCA) was used as a matrix in THF (10 mg/mL). Polymer samples were dissolved in THF/MeOH (1:1, 10 mg/mL), and analyte solutions were prepared by mixing 10 μL of matrix and 1 μL of the polymer sample. Samples were applied using the dried droplet method.

To determine the dispersity of the polymers ($Đ$), size exclusion chromatography (SEC) was performed on an automated Shimadzu HPLC system, with a PLgel 5 μm MIXED-D column at 50 °C, using *N*,*N*-dimethyl acetamide (DMA) containing 50 mM LiCl as the eluent at a flow rate of 0.6 mL/min. Dispersity values were calculated against poly(methyl methacrylate) standards.

**2.4. Isothermal Titration Calorimetry (ITC).** We used isothermal titration calorimetry to obtain full thermodynamic descriptions, i.e., the binding constant ($K_{Ca^{2+}}$), enthalpy ($\Delta H$), and entropy ($\Delta S$), for the interaction between POx-Ale and calcium cations. ITC experiments were carried out on a fully automated Microcal Auto-iTC200. Curve fitting was performed by Origin 6.0 using one set of site-binding model to obtain values for $K$ and $\Delta H$. From these values, $\Delta G$ and $\Delta S$ were calculated using the following equation

$$\Delta G = -RT \ln K = \Delta H - T\Delta S$$

where $R$ is the ideal gas constant, $T$ is the absolute temperature, and $\Delta G$ is the Gibbs free energy. Generally, 0.36 mM per unit of alendronate present in the polymer in Milli-Q water was titrated with 4 mM $CaCl_2$ in Milli-Q water at 20 °C. All polymers were titrated with the same batch of calcium chloride solution. Each ITC titration consisted of 19 injections. All measurements were performed in triplicate.

**2.5. Preparation of Hydrogels.** Gels were prepared by mixing equal volumes (2 × 100 μL) of POx-Ale in phosphate-buffered saline (PBS) and $CaCl_2$ solutions in Milli-Q water. Final polymer concentrations (10, 20, 30 wt %) and calcium concentrations (1, 10, 20, 40 wt %) were obtained within a fixed total volume of 200 μL. The mixtures were stirred vigorously using vortexing for 15 s to obtain homogeneous gels.

**2.6. Rheological Characterizations.** Rheological properties of the gels formed from 30 wt % POx-Ale and 20 wt % $CaCl_2$ were evaluated using an AR2000 advanced rheometer (TA instruments) with a flat steel plate geometry (8 mm diameter) and a fixed gap distance of 500 μm at 25 °C. Frequency sweeps were performed by varying the angular frequency from 0.1 to 10 Hz at a constant strain of 1%. Storage modulus ($G'$), loss modulus ($G''$), and loss tangent ($\tan\delta$) were determined by carrying out a time sweep measurement at 1% strain and 1 Hz. The self-healing ability of the hydrogels was evaluated after three consecutive failure-recovery tests by measuring the recovery of $G'$ after severe gel destruction. First, time sweeps were carried out for 10 min at 1% strain and 1 Hz to determine the viscoelastic region. Then, strain was increased gradually for 3 min from 1 to 1000% to ensure severe network destruction. Subsequently, strain was reduced to 1% for 10 min and the recovery was calculated using the following equation

$$\text{recovery (\%)} = \left(\frac{G'_r}{G'_i}\right)\times 100$$

where $G'_i$ is the average $G'$ during the first time sweep and $G'_r$ is the average $G'$ at the second time sweep. The yield strain (%) of the gels was determined as the crossing point of $G'$ and $G''$ during strain sweep measurements from 1 to 1000% at a frequency of 1 Hz. All measurements were performed in triplicate.

**2.7. Scanning Electron Microscopy/Energy-Dispersive X-ray Spectroscopy.** A field emission scanning electron microscope (SEM; Zeiss Sigma 300) equipped with an energy-dispersive X-ray analyzer (EDX; XFlash detector 610M, Brucker Nano GmbH) was used to evaluate the morphology of gels and perform elemental mapping of Ca using EDX. For the experiment, gels were lyophilized, placed on carbon tape, and sputter-coated with a layer of chromium (10 nm).

**2.8. Visual Observation of Self-Healing Behavior.** Self-healing properties of the hydrogels were evaluated visually. Two gels were colored using either blue (Brilliant) or red (Amaranth) dyes to facilitate visual inspection. They were cut transversally in half, and then, two halves dyed with different colors were brought back together without applying any external force to facilitate visual inspection of their interface.

**2.9. In Vitro Stability of the Hydrogels.** To study both the stability and the reversibility of the formed cross-links, gels were soaked in ethylene diamine tetraacetic acid (EDTA, 100 mM, pH 6) and monitored visually up to 48 h. Vials containing the gels in EDTA were turned around to facilitate the visual inspection of their stability.

**2.10. Statistics.** The statistical analyses were performed using GraphPad InStat software. Rheological results were analyzed statistically using a one-way analysis of variance test, followed by Tukey's multiple comparison test. The significance threshold was set at $P < 0.05$.



DOI: 10.1021/acs.biomac.9b00104
*Biomacromolecules* 2019, 20, 2913−2921

Table 1. Analytical Data of the Synthesized POx-Ale Polymers and the Conversion of Alendronate Functionalization

| | | $^1$H NMR (mol %) | | | | | $M_n$ (kDa) | | |
|---|---|---|---|---|---|---|---|---|---|
| | polymer | EtOx/PropOx | OH | COOH | Ale | conversion (%) | theor.[a] | MALDI-TOF MS | $Đ$ |
| **P1e** | P(EtOx-Ale) | 90 | | 1 | 9 | 90 | 12.8 | 12.0 | 1.11 |
| **P2e** | P(EtOx-Ale) | 80 | | 1 | 19 | 95 | 15.8 | 15.0 | 1.17 |
| **P3e** | P(EtOx-Ale) | 70 | | 2 | 28 | 93 | 19.1 | 19.5 | 1.11 |
| **P6e** | P(EtOx-OH-Ale) | 70 | 21 | 1 | 8 | 89 | 13.1 | 12.6 | 1.11 |
| **P7e** | P(EtOx-OH-Ale) | 70 | 12 | 2 | 16 | 89 | 15.5 | 14.6 | 1.11 |
| **P10e** | P(EtOx-COOH-Ale) | 70 | | 17 | 13 | 100 | 15.9 | 16.3 | 1.11 |
| **P11e** | P(EtOx-COOH-Ale) | 70 | | 10 | 20 | 100 | 17.4 | 16.3 | 1.11 |
| **P4e** | P(PropOx-Ale) | 90 | | 1 | 9 | 90 | 13.4 | 12.2 | 1.08 |
| **P5e** | P(PropOx-Ale) | 70 | | 3 | 27 | 90 | 20.4 | 17.5 | 1.12 |
| **P8e** | P(PropOx-OH-Ale) | 70 | 20 | 1 | 9 | 90 | 14.7 | 12.8 | 1.12 |
| **P9e** | P(PropOx-OH-Ale) | 70 | 10 | 3 | 17 | 85 | 17.4 | 17.9 | 1.12 |
| **P12e** | P(PropOx-COOH-Ale) | 70 | | 22 | 8 | 80 | 16.3 | 14.8 | 1.12 |
| **P13e** | P(PropOx-COOH-Ale) | 70 | | 10 | 20 | 100 | 18.9 | 17.0 | 1.12 |

[a]Theoretical values were calculated considering the polymerization degree of MestOx-functionalized polymers obtained by MALDI-TOF MS and the ratios of the different moieties obtained by $^1$H NMR spectroscopy.

## 3. RESULTS AND DISCUSSION

**3.1. Synthesis of Alendronate-Functionalized Poly(2-oxazoline)s.** We selected alendronate moieties as the reactive groups in view of their strong binding affinity for calcium cations as present in calcium phosphate nanocrystals, the major component of bone tissue.[17,18] In addition, we varied the amount of alendronate, hydroxyl, and carboxylic acid side groups to precisely tune the calcium-binding properties of our polymers, since hydroxyl and carboxylic acid side groups can also interact with calcium cations.

The synthetic route consisted of five steps, as depicted in Scheme 1: (a) polymerization: synthesis of methyl ester-functionalized polymers **P1a−P5a**, (b) synthesis of hydroxyl-functionalized polymers **P1b−P5b**, (c) synthesis of carboxylic acid-functionalized polymers **P1c−P9c**, (d) synthesis of *N*-hydroxysuccinimide-functionalized polymers **P1d−P9d**, and (e) synthesis of alendronate-functionalized polymers **P1e−P13e**.

We used MestOx as a monomer since its methyl ester can be used for chemical functionalization through direct amidation.[29] MestOx was copolymerized with either EtOx or PropOx via CROP to yield statistical copolymers with near-random monomer distribution with different polarity[30−33] and a degree of polymerization of 100. Polymerizations proceeded smoothly, in line with previous results,[28] yielding the desired polymers **P1a−P5a** in multigram scale with a dispersity of 1.1 or 1.2 determined by SEC. Next, MestOx was modified by an amidation reaction with 2-aminoethanol, yielding copolymers with a hydroxyl moiety in the side chain **P1b−P5b**. These hydroxyl groups were either fully or partially converted to carboxylic acid moieties using succinic anhydride **P1c−P9c**, which in turn were subsequently modified into reactive esters by carbodiimide coupling with NHS, yielding **P1d−P9d**. This synthetic route allows for potential in vivo degradation since hydrolytically sensitive esters are introduced in the side chain of the polymer. Finally, alendronate moieties were incorporated in the polymer side chains by a post-polymerization amidation reaction. Since alendronate is not soluble in common organic solvents but soluble in aqueous solutions at neutral and basic pH values, its coupling to the polymers was performed in PBS buffer. However, in water, the coupling of alendronate competes with the hydrolysis of NHS esters and the rates of both reactions increase with the pH. To minimize premature hydrolysis of NHS esters, we carried out the reaction at a pH of 7.4 in cool PBS buffer[21] by adding NHS, EDC, and subsequently the NHS-functionalized polymer in portions, yielding **P1e−P13e**. The conversion of the reaction was slightly higher for EtOx (89−100%) than for PropOx (80−100%) polymers, which can be attributed to the higher water solubility of the EtOx polymer in comparison to that of PropOx. All unreacted NHS moieties were hydrolyzed to COOH as determined by $^1$H NMR spectroscopy.

The synthesized polymers were analyzed with regard to the amount of alendronate (Ale), hydroxyl (OH), and carboxyl (COOH) groups present in the polymer. We were able to precisely control the polymerization parameters (monomer ratios and degree of polymerization) and functionalization degrees. Table 1 summarizes the analytical data of the synthesized POx-Ale polymers.

Detailed experimental procedures and characterization of the synthesized polymers are described in S1. $^1$H and $^{31}$P NMR and MALDI-TOF MS spectra are presented in Figures S1 and S2, respectively.

**3.2. Isothermal Titration Calorimetry (ITC).** ITC was used to assess the affinity between the synthesized POx-Ale polymers and dissolved calcium cations in water. Figure 1 shows representative binding profiles of $Ca^{2+}$ to P($EtOx_{80}$-$Ale_{20}$), sodium alendronate, P($EtOx_{70}$-$COOH_{30}$), and P($EtOx_{70}$-$OH_{30}$) to allow a direct comparison of P($EtOx_{80}$-$Ale_{20}$) with the positive (sodium alendronate) and negative controls (alendronate-free POx-COOH and POx-OH). Binding of calcium cations with free alendronate was considerably weaker (up to 30-fold) than with alendronate groups conjugated to the polymers ($K_{Ca}^{2+}$ = 2.4 × $10^5$ $M^{-1}$), whereas the binding constants of both POx-COOH and POx-OH were below the detection limit.

From Figure 1A, it can be observed that all interactions of POx-Ale were endothermic upon titration of calcium cations to the polymer solution. The enthalpy ($\Delta H$) reached zero when all of the polymers were saturated with calcium. The enthalpy ($\Delta H$) and entropy ($\Delta S$) of binding were similar in all cases, and all interactions were entropically driven, meaning that the complex formation occurs because of a high positive $\Delta S$ due to the release of water as well as counterions. Thermodynamic parameters, i.e., the binding constant $K_{Ca}^{2+}$, enthalpy $\Delta H$, and entropy $\Delta S$ of the binding interaction between POx-Ale and



DOI: 10.1021/acs.biomac.9b00104
Biomacromolecules 2019, 20, 2913−2921

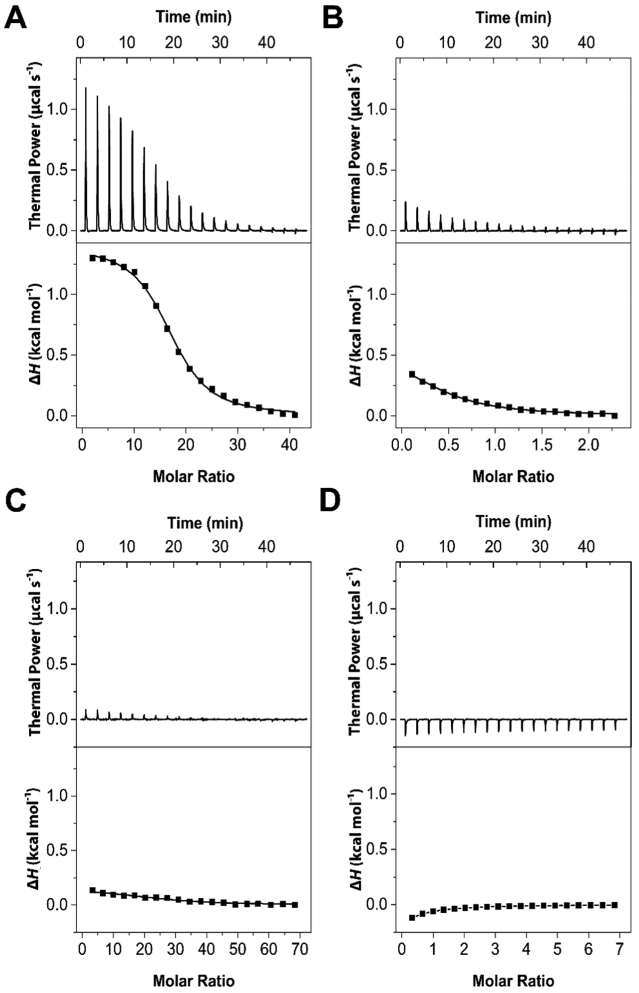


**Figure 1.** ITC profiles showing the association of calcium cations with (A) P($EtOx_{80}$-$Ale_{20}$), (B) alendronate monosodium trihydrate, (C) P($EtOx_{70}$-$COOH_{30}$), and (D) P($EtOx_{70}$-$OH_{30}$).

$Ca^{2+}$, as well as the stoichiometry of the binding defined as the molar ratio $Ca^{2+}$/POx-Ale, determined by ITC are displayed in the Supporting Information (Table S1).

Alendronate, in its zwitterionic form, creates 2:1 complexes with calcium cations.[34] However, POx-alendronate in solution has two negative charges, indicating that each alendronate attached to the polymer is able to form 1:1 complexes with calcium cations. This was indeed confirmed by comparing the stoichiometry of the binding ($N$) determined by ITC (Table S1) with the mol % of alendronate present in the polymer estimated by $^1$H NMR (Table 1). Both techniques gave approximately the same number of alendronate moieties present in each polymer. A molar ratio of 0.5 ($Ca^{2+}$/Ale) was obtained for sodium alendronate, proving that it indeed formed a 2:1 complex with $Ca^{2+}$.

Polymers containing alendronate moieties clearly showed a strong interaction with calcium cations, as confirmed by their high binding constants ($K_{Ca}^{2+}$). As depicted in Figure 2, the calcium-binding affinity increased linearly with the number of alendronate moieties conjugated to the polymer, corresponding to the molar ratio ($Ca^{2+}$/POx-Ale) determined by ITC. Therefore, the linear increase with the amount of alendronate shows that there is no specific cooperative effect of having multiple alendronate moieties conjugated to the same backbone.

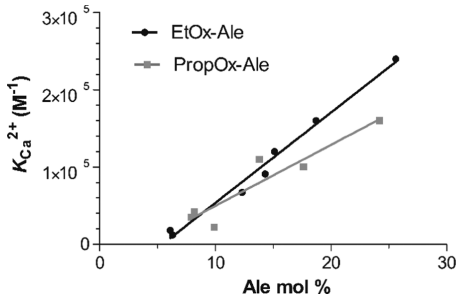


**Figure 2.** Binding affinity of POx-Ale with $Ca^{2+}$ ($K_{Ca}^{2+}$) vs the mol % of alendronate (Ale) present in the polymer.

Furthermore, the interaction of EtOx polymers with $Ca^{2+}$ was 1.5-fold higher than that of PropOx polymers, which might be caused by the higher solubility of hydrophilic EtOx polymers in aqueous solutions compared to more hydrophobic PropOx, thereby increasing their reactivity. Notably, P($EtOx_{70}$-$Ale_{30}$) showed the highest binding affinity for calcium cations, which was substantially higher than calcium-binding affinities reported previously for polymers such as alginate (25-fold increase, $K_{Ca}^{2+}$ = 1.0 × $10^4$ $M^{-1}$) and alendronate-conjugated poly(ethylene glycol) polymers (PEG-Ale) (120-fold increase, $K_{Ca}^{2+}$ = 2.0 × $10^3$ $M^{-1}$).[35,36] The higher binding affinity of POx-Ale as compared to that of alginate was attributed to the superior affinity of alendronate vs carboxylic acid groups for calcium cations.[35] The main cause of the significantly enhanced affinity of POx-Ale polymers to calcium compared to that of PEG-Ale is a result of having multiple alendronates along the polymer backbone (30 mol % for POx-Ale and 2 mol % for PEG-Ale), which obviously leads to improved binding. As shown in Figure 2, the type of backbone also plays a role, albeit minor compared to the number of alendronates.

Due to the slightly higher calcium-binding affinity of P(EtOx-Ale) vs P(PropOx-Ale), their higher solubility in aqueous solutions, and their higher conversion, EtOx-based polymers were selected for further studies.

**3.3. Visual Observation of Gelation.** Mixing equal volumes of alendronate-functionalized polymers and $Ca^{2+}$ solutions yielded either liquids, viscous solutions, transparent gels, or white gels (see Table S2 for more details). Generally, increasing both polymer and calcium concentrations formed stronger gels. Alendronate-free polymers containing either hydroxyl (P($EtOx_{70}$-$OH_{30}$)) or carboxylic acid (P($EtOx_{70}$-$COOH_{30}$)) moieties in the side chains were used as negative controls. These polymers did not form gels upon mixing with calcium solutions at any of the concentrations tested, which confirms that alendronate moieties were responsible for the formation of cross-linked hydrogel networks. Based on data in Table S2, concentrations of 30 wt % of polymer and 20 wt % of $Ca^{2+}$ were selected for further rheological studies.

First, we investigated how the additional presence of hydroxyl or carboxyl acid moieties, in combination with alendronate, affected the process of network formation. For this purpose, three types of gels were created: P($EtOx_{70}$-$Ale_{30}$) and P($EtOx_{70}$-$COOH_{10}$-$Ale_{20}$) yielded white stable networks, whereas P-($EtOx_{70}$-$OH_{10}$-$Ale_{20}$) formed transparent soft gels. We attribute this difference to the very fast gelation of P($EtOx_{70}$-$Ale_{30}$) and P($EtOx_{70}$-$COOH_{10}$-$Ale_{20}$) polymers due to the energetically favorable interactions of alendronate and carboxylic acid moieties with calcium cations, thereby resulting in the formation of precipitates. These precipitates induced light scattering,


DOI: 10.1021/acs.biomac.9b00104
Biomacromolecules 2019, 20, 2913−2921

hence creating a white appearance. The transparent appearance of gels containing hydroxyl moieties may be related to the better hydration of these gels since, as opposed to alendronate and carboxylic acid moieties, hydroxyl groups were less involved in calcium binding.

To prove the formation of these precipitates, the morphology of the hydrogels was further investigated using electron microscopy and elemental mapping by means of EDX. Figure S3 shows the corresponding scanning electron micrographs, indicating a homogeneous distribution of $Ca^{2+}$, which confirms again that gel formation relied on strong noncovalent interactions between POx-Ale and $Ca^{2+}$. Precipitates were indeed observed in hydrogels comprising polymers with strongest affinity for calcium cations ($P(EtOx_{70}\text{-}Ale_{30})$) and to a lesser extent also in gels containing polymers of intermediate affinity for calcium ($P(EtOx_{70}\text{-}COOH_{10}\text{-}Ale_{20})$). This phenomenon was caused by their very fast gelation. The gelation kinetics of $P(EtOx_{70}\text{-}OH_{10}\text{-}Ale_{20})$ was considerably slower than that of other two polymers due to their lower affinity for calcium, resulting in more homogeneous gels without any precipitates.

**3.4. Rheological Characterization.** We hypothesized that the ability of POx-Ale polymers to form calcium-cross-linked networks would depend on the number of alendronate moieties present in the polymer. In general, increasing the number of alendronate moieties in the polymer increased the stiffness of the resulting gels, as reflected by the increase in the storage modulus ($G'$) with increasing alendronate content (Figure 3A). $P(EtOx_{90}\text{-}Ale_{10})$, $P(EtOx_{80}\text{-}Ale_{20})$, and $P(EtOx_{70}\text{-}OH_{20}\text{-}Ale_{10})$ produced weak liquidlike gels ($\tan\delta$ = 1.05, 1.06, and 1.51, respectively), whereas more robust and solidlike hydrogels were formed at a higher alendronate concentration of 30 mol % ($P(EtOx_{70}\text{-}Ale_{30})$, $\tan\delta$ = 0.41). Remarkably, the storage modulus of the hydrogels increased 60-fold by enhancing the amount of alendronate substitution degree from 10 to 20% and more than 7000-fold by increasing the alendronate substitution degree from 10 to 30%. These results confirm that the presence of alendronate was crucial for formation of stiff and robust calcium-cross-linked hydrogels. In addition, simultaneous presence of carboxylic acid moieties in the side chain of the polymer increased the stiffness of alendronate-functionalized POx hydrogels of similar alendronate content. The introduction of hydroxyl groups, on the other hand, increased the malleability of alendronate-functionalized POx hydrogels of similar alendronate content, revealing higher yield strain values.

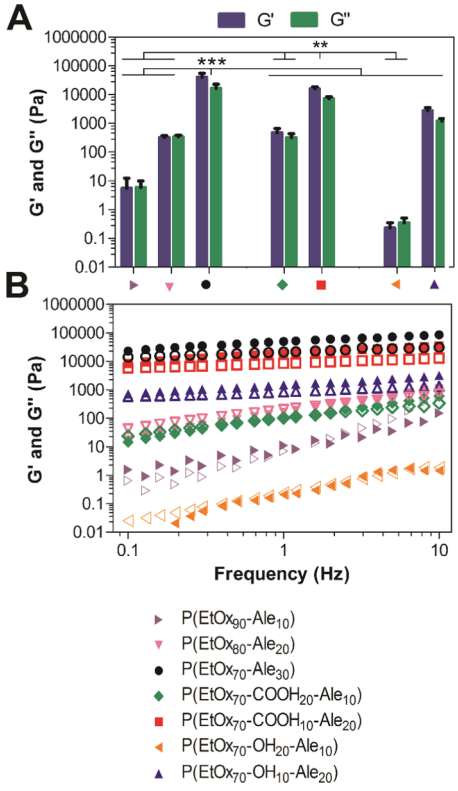


**Figure 3.** (A) Storage ($G'$) and loss ($G''$) moduli of hydrogels formed from 30 wt % alendronate-functionalized POxs and 20 wt % $CaCl_2$, measured at a frequency of 1 Hz. (B) Frequency dependence of storage (solid symbols, $G'$) and loss (open symbols, $G''$) moduli at 1% strain of hydrogels formed from 30 wt % alendronate-functionalized POxs and 20 wt % $CaCl_2$.

Generally, the stiffness of all gel networks increased with increasing oscillatory frequency (see Figure 3B). All gels displayed solidlike behavior (characterized by storage modulus values ($G'$) higher than loss modulus ($G''$)) over the entire frequency range, behaving similarly to permanent networks, except for 10 mol % alendronate POxs.

The three polymers with the highest $G'$ values, i.e., $P(EtOx_{70}\text{-}Ale_{30})$, $P(EtOx_{70}\text{-}COOH_{10}\text{-}Ale_{20})$, and $P(EtOx_{70}\text{-}OH_{10}\text{-}Ale_{20})$, were further analyzed in more detail as a function of polymer and calcium concentrations.

**3.5. Effect of Polymer and Calcium Concentration on Viscoelastic Properties.** The effect of polymer concentration was studied at a constant calcium concentration of 20 wt % (Figure 4A, B). As expected, an increase in polymer concentration resulted in a significantly increased storage modulus (Figure 4A). $\tan\delta$ values of polymers containing hydroxyl groups ($P(EtOx_{70}\text{-}OH_{10}\text{-}Ale_{20})$) decreased with the increased polymer concentration, whereas $\tan\delta$ of hydroxyl-free polymers did not depend on the polymer concentration of the cross-linked networks (Figure 4B). These results indicate that hydroxyl side groups also contributed to the formation of robust cross-linked networks.

The effect of calcium concentration was studied at a constant polymer concentration of 30 wt % (Figure 4C, D). The storage modulus increased significantly for all polymers by enhancing the calcium content from 10 to 20 wt %, which corresponded to a transition from liquidlike to solidlike behavior. These results confirm that the number of interactions between $Ca^{2+}$ and alendronate was critical for the formation of strong, yet reversible, networks. However, $G'$ values declined from 15.8 to 2.6 kPa for $P(EtOx_{70}\text{-}COOH_{10}\text{-}Ale_{20})$ and from 40.3 to 1.9 kPa for $P(EtOx_{70}\text{-}Ale_{30})$ upon a further increase of the calcium concentration from 20 to 40 wt %, whereas the storage modulus of $P(EtOx_{70}\text{-}OH_{10}\text{-}Ale_{20})$ remained constant at a value of about 1.7 kPa (Figure 4C). This might be related to the better hydration properties of hydroxyl-containing polymers, since their binding to calcium is weaker than for those not containing hydroxyl moieties. Calcium induces cross-linking up to 20 wt % for $P(EtOx_{70}\text{-}COOH_{10}\text{-}Ale_{20})$ and $P(EtOx_{70}\text{-}Ale_{30})$, but this is disrupted when the concentration of $Ca^{2+}$ is too high. Due to calcium saturation, each alendronate is occupied with two calcium ions (one in each phosphonate group) and there is less chance of interaction of one alendronate (two phosphonates) with one calcium. The $\tan\delta$ values increased with the calcium content for $P(EtOx_{70}\text{-}COOH_{10}\text{-}Ale_{20})$ and $P(EtOx_{70}\text{-}Ale_{30})$ (Figure 4D), which also indicates that viscous behavior was more prominent for hydrogels with excessive calcium contents.



DOI: 10.1021/acs.biomac.9b00104
Biomacromolecules 2019, 20, 2913−2921

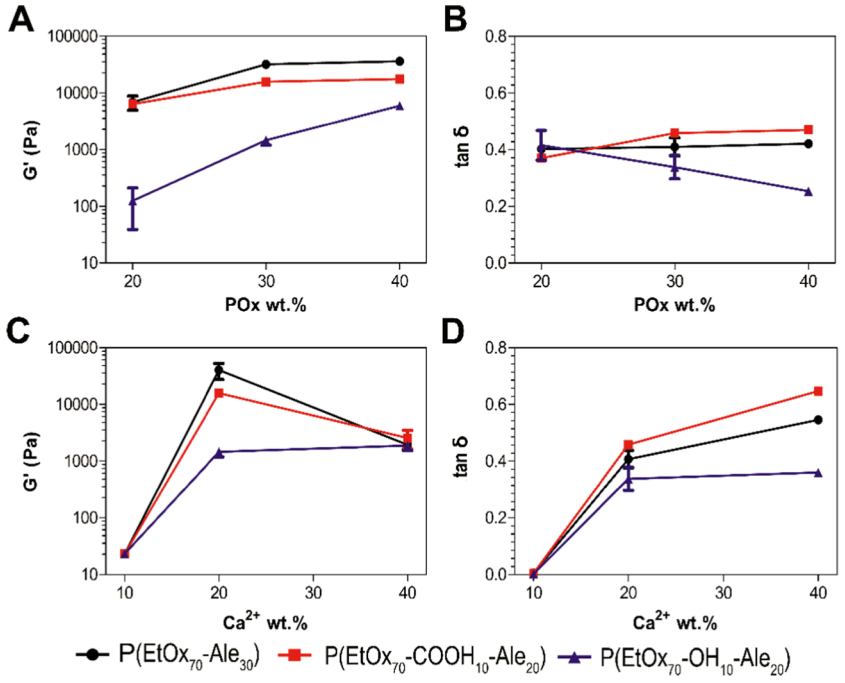


**Figure 4.** (A) Storage modulus ($G'$) and (B) tan $\delta$ of hydrogels formed from several polymer concentrations and 20 wt % $CaCl_2$. (C) Storage modulus ($G'$) and (D) tan $\delta$ of hydrogels formed from 20 wt % $CaCl_2$ and several polymer concentrations. Most error bars fall within the data points.

However, as expected, the tan $\delta$ values for P(EtOx$_{70}$-OH$_{10}$-Ale$_{20}$) remained constant on increasing the calcium concentration from 20 to 40 wt %.

**3.6. Self-Healing Behavior.** Figure 5 depicts the self-healing ability of the networks upon gel destruction induced by transversal cutting of the gel. Two gels were stained with either red or blue dyes, cut in half, after which gel pieces with different colors were brought back together without applying any external force. After 2 min of contact, the two pieces adhered tightly without any viscous flow, and their connection was strong enough to allow for both stretching by gravity and manual stretching.

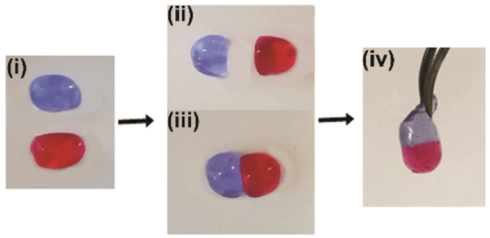


**Figure 5.** Self-healing behavior of a hydrogel composed of 30 wt % P(EtOx$_{70}$-OH$_{10}$-Ale$_{20}$) and 20 wt % $Ca^{2+}$ showing (i) original stained hydrogels, (ii) hydrogels after cutting, (iii) hydrogels brought back together without applying external force, and (iv) self-healed hydrogel.

This qualitative observation of the self-healing behavior of our hydrogels was confirmed quantitatively by rheological analysis (Figure 6). During these experiments, oscillatory strain was increased from 1 to 1000% in 3 min to induce gel failure ($G' < G''$ corresponding to tan $\delta > 1$). After severe network destruction, a very fast recovery of the storage modulus was observed after reducing the strain back to its initial value (1%) (Figure 6). Surprisingly, the storage modulus of the three hydrogels exceeded the initial value after destructive shearing, resulting into a self-healing capacity of more than 100%. This strong self-healing capacity can be explained by the fact that diffusion of the polymer chains and calcium cations increased during the destructive phase, thereby improving the cross-linking homogeneity and density. This effect was most pronounced for P(EtOx$_{70}$-Ale$_{30}$) as this gel was initially less homogeneous and more brittle than the other two hydrogels containing either hydroxyl or carboxylic acid groups. Moreover, for P(EtOx$_{70}$-Ale$_{30}$), the self-healing capacity declined from around 150% after cycle one to 100% after cycle three, whereas it remained at a more constant value between 100 and 120% for the other two hydrogels for all three destructive shearing cycles (Figure 6B). Figure 6C shows the yield strain of the three hydrogels after three consecutive network destructions. Hydrogels made of hydroxyl-containing polymers were more flexible and revealed higher yield strain values, whereas hydroxyl-free gels (P(EtOx$_{70}$-COOH$_{10}$-Ale$_{20}$) and P(EtOx$_{70}$-Ale$_{30}$)) were more brittle. However, the yield strain was not affected by repeated network destruction, stressing the strong capacity of POx-Ale-based hydrogel networks.

**3.7. In Vitro Stability of the Hydrogels.** The in vitro stability of the POx-Ale-based hydrogels was studied as a function of their soaking time in a solution containing a strong calcium chelator, i.e., 100 mM EDTA at pH 6. P(EtOx$_{70}$-OH$_{10}$-Ale$_{20}$) was completely dissolved in EDTA after 3 h of immersion, which confirmed that the cross-links between $Ca^{2+}$ and alendronate were responsible for network formation. However, both P(EtOx$_{70}$-Ale$_{30}$) and P(EtOx$_{70}$-COOH$_{10}$-Ale$_{20}$) remained stable even after 48 h of soaking in EDTA, which means that the affinity of calcium for these polymers was higher than the affinity for EDTA (see Figure S4), which again stresses the exceptionally strong affinity of our polymers for $Ca^{2+}$.

## 4. CONCLUSIONS

A novel library of alendronate-functionalized POxs was successfully synthesized with control over the polymerization and functionalization degrees. We demonstrated much higher



DOI: 10.1021/acs.biomac.9b00104
Biomacromolecules 2019, 20, 2913−2921

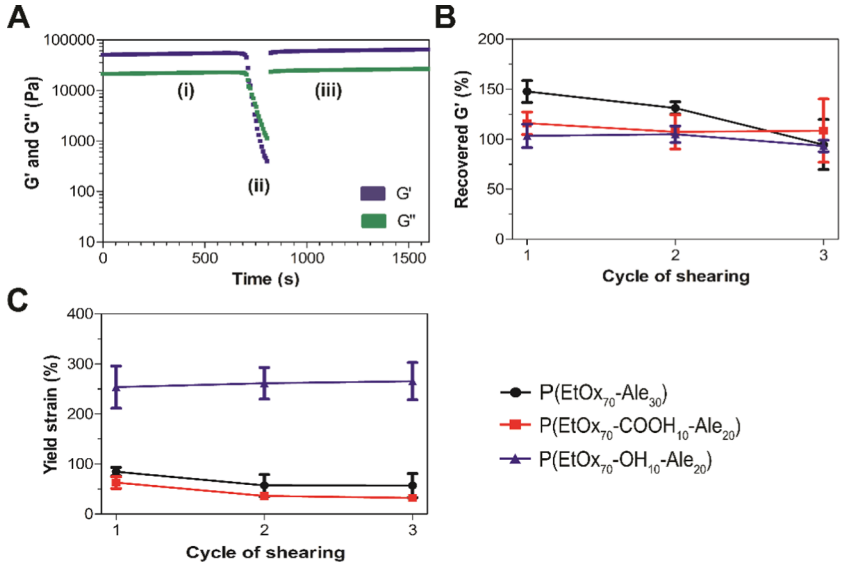


**Figure 6.** (A) Rheological analysis of the self-healing behavior of a hydrogel composed of 30 wt % P($EtOx_{70}$-$Ale_{30}$) and 20 wt % $Ca^{2+}$ upon destructive network shearing in three steps: (i) time sweep at 1% strain, (ii) network destruction by increasing strain from 1 to 1000%, and (iii) recovery at 1% strain. (B) Recovery of stiffness ($G'$) after three consecutive network destructions. (C) Yield strain during three consecutive network destructions.

binding affinity of these polymers for calcium cations in comparison with other calcium-binding polymers reported previously.[35,36] Results showed that adjusting the alendronate content in the polymer produced robust gels with a strong capacity for self-healing. The tunable synthetic versatility and affinity for calcium render these polymers excellent candidates for various applications in biomedicine.

## ■ ASSOCIATED CONTENT

### Supporting Information

The Supporting Information is available free of charge on the ACS Publications website at DOI: 10.1021/acs.biomac.9b00104.

Experimental procedures and characterization of the synthesized polymers (Table S1); $^{1}H$ and $^{31}P$ NMR and MALDI-TOF MS spectra (Figures S1 and S2, respectively); thermodynamic parameters of the binding interaction between POx-Ale and $Ca^{2+}$ determined by ITC (Table S1); visual screening of gelation at different polymer and $CaCl_2$ concentrations and scanning electron micrographs with elemental mapping for calcium (Table S2 and Figure S3, respectively); and in vitro stability of the hydrogels in EDTA (Figure S4) (PDF)

## ■ AUTHOR INFORMATION


### Corresponding Authors

*E-mail: Sander.Leeuwenburgh@radboudumc.nl (S. C. G. L.).
*E-mail: J.C.M.v.Hest@tue.nl (J. C. M. v. H.).

### ORCID

Fang Yang: 0000-0002-4022-7643
Jasmin Mecinović: 0000-0002-5559-3822
Sander C. G. Leeuwenburgh: 0000-0003-1471-6133
Jan C. M. van Hest: 0000-0001-7973-2404

### Present Address

#Department of Physics, Chemistry and Pharmacy, University of Southern Denmark, 5230 Odense, Denmark (J. M.).

### Author Contributions

⊥S. C. G. L. and J. C. M. v. H. contributed equally to this work.


### Notes

The authors declare the following competing financial interest(s): This work has been performed in collaboration with Johan C. M. E. Bender, CEO GATT Technologies BV. Sander C. G. Leeuwenburgh and Jan C. M. van Hest are scientific advisors of GATT Technologies BV.

## ■ ACKNOWLEDGMENTS

Erik Koeken and Dustin van Doeselaar are acknowledged for their help on polymer synthesis. We acknowledge financial support from the Netherlands Organization for Scientific Research (NWO) and GATT Technologies BV (grant number 14435).

## ■ REFERENCES


(1) Tomalia, D. A.; Sheetz, D. P. Homopolymerization of 2-Alkyl- and 2-Aryl-2-oxazolines. *J. Polym. Sci., Part A-1: Polym. Chem.* **1966**, *4*, 2253−2265.

(2) Seeliger, W.; Aufderhaar, E.; Diepers, W.; Feinauer, R.; Nehring, R.; Thier, W.; Hellmann, H. Recent Syntheses and Reactions of Cyclic Imidic Esters. *Angew. Chem., Int. Ed.* **1966**, *5*, 875−888.

(3) Kagiya, T.; Narisawa, S.; Maeda, T.; Fukui, K. Ring-Opening Polymerization of 2-Substituted 2-Oxazolines. *J. Polym. Sci., Part B: Polym. Lett.* **1966**, *4*, 441−445.

(4) Bassiri, T. G.; Levy, A.; Litt, M. Polymerization of Cyclic Imino Ethers. I. Oxazolines. *J. Polym. Sci., Part B: Polym. Lett* **1967**, *5*, 871−879.

(5) Adams, N.; Schubert, U. S. Poly(2-oxazolines) in Biological and Biomedical Application Contexts. *Adv. Drug Delivery Rev.* **2007**, *59*, 1504−1520.

(6) de la Rosa, V. R. Poly(2-oxazoline)s as Materials for Biomedical Applications. *J. Mater. Sci.: Mater. Med.* **2014**, *25*, 1211−1225.

(7) Sedlacek, O.; Monnery, B. D.; Filippov, S. K.; Hoogenboom, R.; Hruby, M. Poly(2-oxazoline)s: Are They More Advantageous for Biomedical Applications than Other Polymers? *Macromol. Rapid Commun.* **2012**, *33*, 1648−1662.

(8) Grube, M.; Leiske, M. N.; Schubert, U. S.; Nischang, I. POx as an Alternative to PEG? A Hydrodynamic and Light Scattering Study. *Macromolecules* **2018**, *51*, 1905−1916.

(9) Barz, M.; Luxenhofer, R.; Zentel, R.; Vicent, M. J. Overcoming the PEG-Addiction: Well-Defined Alternatives to PEG, from Structure-




DOI: 10.1021/acs.biomac.9b00104
*Biomacromolecules* 2019, 20, 2913−2921

Property Relationships to Better Defined Therapeutics. *Polym. Chem.* **2011**, *2*, 1900−1918.
(10) Hoogenboom, R. Poly(2-oxazoline)s: A Polymer Class with Numerous Potential Applications. *Angew. Chem., Int. Ed.* **2009**, *48*, 7978−7994.
(11) Guillerm, B.; Monge, S.; Lapinte, V.; Robin, J. How to Modulate the Chemical Structure of Polyoxazolines by Appropriate Functionalization. *Macromol. Rapid Commun.* **2012**, *33*, 1600−1612.
(12) Lava, K.; Verbraeken, B.; Hoogenboom, R. Poly(2-oxazoline)s and Click Chemistry: a Versatile Toolbox toward Multi-Functional Polymers. *Eur. Polym. J.* **2015**, *65*, 98−111.
(13) Russell, R. G. Bisphosphonates: The First 40 Years. *Bone* **2011**, *49*, 2−19.
(14) Gatti, D.; Adami, S. New Bisphosphonates in the Treatment of Bone Diseases. *Drugs Aging* **1999**, *15*, 285−296.
(15) Lewiecki, E. M. Bisphosphonates for the Treatment of Osteoporosis: Insights for Clinicians. *Ther. Adv. Chronic Dis.* **2010**, *1*, 115−128.
(16) Drake, M. T.; Clarke, B. L.; Khosla, S. Bisphosphonates: Mechanism of Action and Role in Clinical Practice. *Mayo Clin. Proc.* **2008**, *83*, 1032−1045.
(17) Wang, D.; Miller, S. C.; Kopeckova, P.; Kopecek, J. Bone-Targeting Macromolecular Therapeutics. *Adv. Drug Delivery Rev.* **2005**, *57*, 1049−1076.
(18) Rodan, G. A.; Fleisch, H. A. Bisphosphonates: Mechanisms of Action. *J. Clin. Invest.* **1996**, *97*, 2692−2696.
(19) Boanini, E.; Gazzano, M.; Rubini, K.; Bigi, A. Composite Nanocrystals Provide New Insight on Alendronate Interaction with Hydroxyapatite Structure. *Adv. Mater.* **2007**, *19*, 2499−2502.
(20) Errassifi, F.; Sarda, S.; Barroug, A.; Legrouri, A.; Sfihi, H.; Rey, C. Infrared, Raman and NMR Investigations of Risedronate Adsorption on Nanocrystalline Apatites. *J. Colloid Interface Sci.* **2014**, *420*, 101−111.
(21) López-Pérez, P. M.; da Silva, R. M. P.; Strehin, I.; Kouwer, P. H. J.; Leeuwenburgh, S. C. G.; Messersmith, P. B. Self-Healing Hydrogels Formed by Complexation between Calcium Ions and Bisphosphonate-Functionalized Star-Shaped Polymers. *Macromolecules* **2017**, *50*, 8698−8706.
(22) Diba, M.; An, J.; Schmidt, S.; Hembury, M.; Ossipov, D.; Boccaccini, A. R.; Leeuwenburgh, S. C. Exploiting Bisphosphonate-Bioactive-Glass Interactions for the Development of Self-Healing and Bioactive Composite Hydrogels. *Macromol. Rapid Commun.* **2016**, *37*, 1952−1959.
(23) Hager, M. D.; Greil, P.; Leyens, C.; van der Zwaag, S.; Schubert, U. S. Self-Healing Materials. *Adv. Mater.* **2010**, *22*, 5424−5430.
(24) Taylor, D. L.; in het Panhuis, M. Self-Healing Hydrogels. *Adv. Mater.* **2016**, *28*, 9060−9093.
(25) Bekas, D. G.; Tsirka, K.; Baltzis, D.; Paipetis, A. S. Self-Healing Materials: A Review of Advances in Materials, Evaluation, Characterization and Monitoring Techniques. *Composites, Part B* **2016**, *87*, 92−119.
(26) Diba, M.; Spaans, S.; Ning, K.; Ippel, B. D.; Yang, F.; Loomans, B.; Dankers, P. Y. W.; Leeuwenburgh, S. C. G. Self-Healing Biomaterials: From Molecular Concepts to Clinical Applications. *Adv. Mater. Interfaces* **2018**, *5*, No. 1800118.
(27) Nejadnik, M. R.; Yang, X.; Bongio, M.; Alghamdi, H. S.; van den Beucken, J. J.; Huysmans, M. C.; Jansen, J. A.; Hilborn, J.; Ossipov, D.; Leeuwenburgh, S. C. Self-Healing Hybrid Nanocomposites Consisting of Bisphosphonated Hyaluronan and Calcium Phosphate Nanoparticles. *Biomaterials* **2014**, *35*, 6918−6929.
(28) Wiesbrock, F.; Hoogenboom, R.; Schubert, U. S. Microwave-Assisted Polymer Synthesis: State-of-the-Art and Future Perspectives. *Macromol. Rapid Commun.* **2004**, *25*, 1739−1764.
(29) Mees, M. A.; Hoogenboom, R. Functional Poly(2-oxazoline)s by Direct Amidation of Methyl Ester Side Chains. *Macromolecules* **2015**, *48*, 3531−3538.
(30) Bouten, P. J. M.; Hertsen, D.; Vergaelen, M.; Monnery, B. D.; Catak, S.; van Hest, J. C. M.; van Speybroeck, V.; Hoogenboom, R. Synthesis of Poly(2-oxazoline)s with Side Chain Methyl Ester Functionalities: Detailed Understanding of Living Copolymerization Behavior of Methyl Ester Containing Monomers with 2-Alkyl-2-oxazolines. *J. Polym. Sci., Part A: Polym. Chem.* **2015**, *53*, 2649−2661.
(31) Boerman, M. A.; van der Laan, H. L.; Bender, J. C. M. E.; Hoogenboom, R.; Jansen, J. A.; Leeuwenburgh, S. C.; van Hest, J. C. M. Synthesis of pH- and Thermoresponsive Poly(2-*n*-propyl-2-oxazoline) Based Copolymers. *J. Polym. Sci., Part A: Polym. Chem.* **2016**, *54*, 1573−1582.
(32) Bouten, P. J. M.; Hertsen, D.; Vergaelen, M.; Monnery, B. D.; Boerman, M. A.; Goossens, H.; Catak, S.; van Hest, J. C. M.; van Speybroeck, V.; Hoogenboom, R. Accelerated Living Cationic Ring-Opening Polymerization of a Methyl Ester Functionalized 2-Oxazoline Monomer. *Polym. Chem.* **2015**, *6*, 514−518.
(33) Boerman, M. A.; Roozen, E.; Sánchez-Fernández, M. J.; Keereweer, A. R.; Félix Lanao, R. P.; Bender, J.; Hoogenboom, R.; Leeuwenburgh, S. C.; Jansen, J. A.; van Goor, H.; van Hest, J. C. M. Next Generation Hemostatic Materials Based on NHS-Ester Functionalized Poly(2-oxazoline)s. *Biomacromolecules* **2017**, *18*, 2529−2538.
(34) Fernández, D.; Vega, D.; Goeta, A. Alendronate Zwitterions Bind to Calcium Cations Arranged in Columns. *Acta Crystallogr., Sect. C: Struct. Chem.* **2003**, *59*, 543−545.
(35) Chu, W.; Huang, Y.; Yang, C.; Liao, Y.; Zhang, X.; Yan, M.; Cui, S.; Zhao, C. Calcium Phosphate Nanoparticles Functionalized with Alendronate-Conjugated Polyethylene Glycol (PEG) for the Treatment of Bone Metastasis. *Int. J. Pharm.* **2017**, *516*, 352−363.
(36) Fang, Y.; Al-Assaf, S.; Phillips, G. O.; Nishinari, K.; Funami, T.; Williams, P. A.; Li, L. Multiple Steps and Critical Behaviors of the Binding of Calcium to Alginate. *J. Phys. Chem. B* **2007**, *111*, 2456−2462.


DOI: 10.1021/acs.biomac.9b00104
*Biomacromolecules* 2019, 20, 2913−2921